

Spectroscopic, Thermal, and Electrical Investigations of PVDF Films Filled with BiCl₃

N. A. Hakeem,¹ H. I. Abdelkader,² N. A. El-sheshtawi,² I. S. Eleshmawi¹

¹*Spectroscopy Department, Physics Division, National Research Center, Dokki, Giza, Egypt*

²*Physics Department, Faculty of Science, Mansoura University, Egypt*

Received 28 June 2005; accepted 7 January 2006

DOI 10.1002/app.24135

Published online in Wiley InterScience (www.interscience.wiley.com).

ABSTRACT: Poly(vinylidene fluoride) (PVDF) films filled with BiCl₃ in the mass fraction range of $0.1 \leq W \leq 10$ were prepared. α - and β -Crystalline PVDF phases were detected and characterized by spectroscopic analysis. Fourier transform infrared analysis detected the presence of α - and β -phase head-to-head and tail-to-tail polymer chain defects. The band detected at 1670 cm^{-1} was assigned to C=C, indicating polarons in the polymeric matrix. The degree of crystallinity increased by increasing the filling level (FL), and the maximum relative β -phase content was found at $w = 5\%$ FL. This result was confirmed by X-ray diffraction (XRD) and differential scanning calorimetry (DSC) analysis. The X-ray analysis confirmed the presence of α and β phases, and

no peaks corresponding to pure BiCl₃ were found. DSC thermograms showed a sharp endothermic peak at $T_1 = 444 \text{ K}$ for different FLs because of the melting. This peak was used to calculate the activation energy and the order of the reaction. The DC electrical resistivity was attributed to the one-dimensional interpolaron hopping mechanism. The FL dependence of $\log \rho$ and hopping distance (R_0) at 373 K was observed, indicating the FL affected the distribution of the hopping sites. © 2006 Wiley Periodicals, Inc. *J Appl Polym Sci* 102: 2125–2131, 2006

Key words: FT-IR; XRD; differential scanning calorimetry (DSC); DC electrical resistivity

INTRODUCTION

PVDF morphology and piezoelectric properties have become subjects of active research in the last three decades.¹ In addition to these properties, PVDF also exhibits at least five crystalline phases, known as form I (β),² form II (α),³ form III (γ),⁴ polar II (α_p),⁵ and polar form III (γ_p).⁶ Form I is distinguished from the others in applications such as piezoelectricity,⁷ pyroelectricity,⁸ ferroelectricity,⁹ microwave modulation,¹⁰ nonlinear optical properties,¹¹ and infrared to visible converter.¹²

The polymer chains of PVDF are packed in the crystal in one of two ways. The dipoles are either parallel, and the crystal possesses a net dipole moment (polar forms β , γ , α_p , and γ_p) or antiparallel, so that the net dipole moment is zero (nonpolar form α).

The crystalline β , γ , α_p , and γ_p phases of PVDF, which are permanently polarized, are ferroelectric. That is the basis of a number of technical applications of this material.

Recent investigations by our research group revealed that metal halide fillers significantly modify the structure and physical properties of PVDF films.^{13–15}

The present work was devoted to studying the effect of BiCl₃ filler on the content of the α - and β phases and the structural and physical properties of PVDF films.

EXPERIMENTAL

PVDF films were prepared by a casting method. PVDF powder (SOLEF 1008) was dissolved in dimethylformamide (DMF). BiCl₃ also was dissolved in DMF. The BiCl₃ solution was added to the dissolved polymer at a suitable viscosity. The mixture was cast to a glass dish and kept in a dry atmosphere at 333 K for 7 days to ensure the removal of the solvent traces. The films had a thickness in the range of $0.11\text{--}0.15 \text{ mm}$. PVDF films were prepared with mass fractions of BiCl₃ of 0.0%, 1.0%, 2.5%, 5.0%, 7.5%, and 10%.

A Fourier transform infrared (FTIR) spectrophotometer (Perkin Elmer 883, Tokyo, Japan) was used to measure the FTIR transmittance spectra in the wave number range of $200\text{--}2000 \text{ cm}^{-1}$. The X-ray diffraction scans were obtained using a Siemens type F diffractometer with Cu K α radiation and a LiF monochromator. JEOL 5300 scanning electron microscope, operating at an accelerating voltage of 15 kV was used to observe the morphology of the PVDF films. The surfaces of the samples were coated with a 3.5-nm layer of gold to minimize sample charging effects from the

Correspondence to: I. S. Eleshmawi (islam_shukri2000@yahoo.com).

electron beam. Differential scanning calorimetry (DSC) for the prepared films was carried out using a Shimadzu-DSC-50 in the temperature range of 398–573 K with a heating rate 5°C/min. The DC electrical resistivity was measured using an insulation tester (level type T M14) whose accuracy was within $\pm 0.2\%$.

RESULTS AND DISCUSSION

Fourier transform infrared analysis

Figure 1 shows the IR spectra of the PVDF films filled with different FLs of BiCl_3 in the 200–2000 cm^{-1} region. The main characteristic peaks of PVDF were observed. The bands at 610, 763, and 879 cm^{-1} corresponded to the α phase, whereas the bands at 420, 510, and 1404 cm^{-1} were a result of the β phase of PVDF.

The peak at 510 cm^{-1} , belonging to the β phase, was assigned to CF_2 bending and CH_2 wagging modes, whereas the peak at 610 cm^{-1} was a result of CF_2 bending and skeletal bending of the α phase.¹⁶

The band at 670 cm^{-1} was taken as a measure of the concentration of the head-to-head [(h-to-h)] and tail-

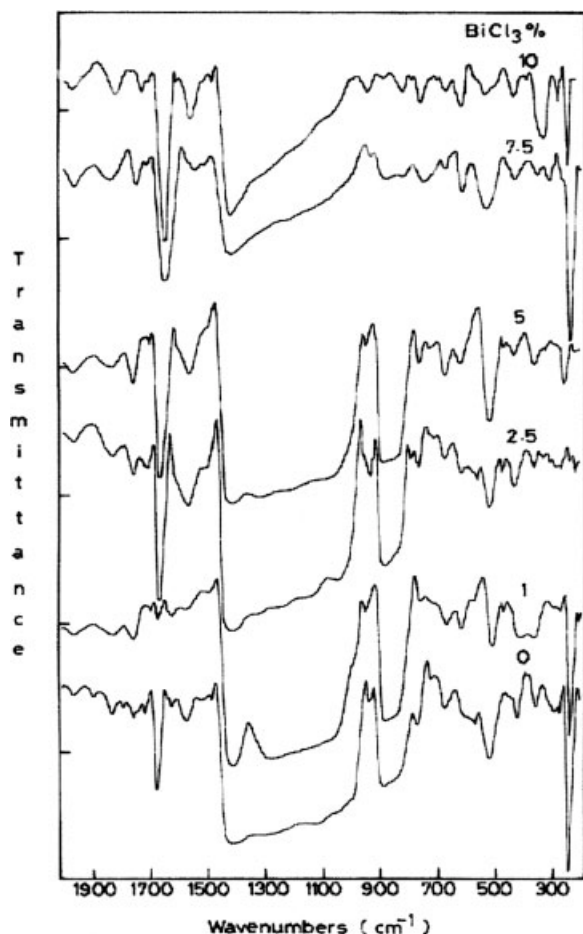


Figure 1 IR transmittance of PVDF filled with different FLs of BiCl_3 .

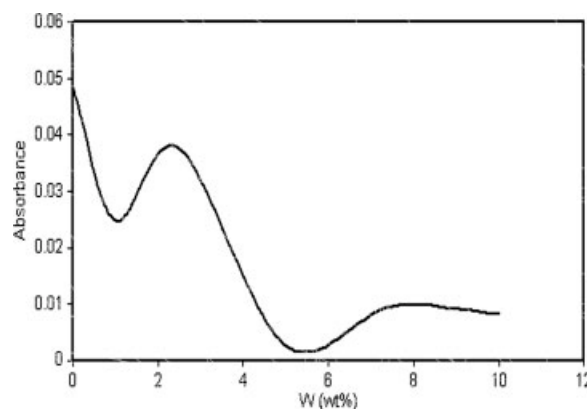


Figure 2 Absorbance FL dependence of the peak intensity at 670 cm^{-1} .

to-tail [(t-to-t)] polymer chain defects.¹⁷ Figure 2 shows the absorbance FL dependence of the peak intensity at 670 cm^{-1} of (h-to-h). It is observed that the maximum and the minimum values of (h-to-h) occurred at 2.5% and 5% FL, respectively.

The IR band appearing at 925 cm^{-1} was assigned to the totally symmetric vibrations of perchlorate anion. This band shifted with FL changes from 925 to 952 cm^{-1} , which means the filler reacted with the polymer matrices.¹⁸

In the IR spectra of the samples under investigation there was a strong and broad band around 1300 cm^{-1} . In partially crystalline samples this amorphous band overlapped the crystalline bands in this region and changed the spectral feature depending on the degree of crystallinity of the sample.¹⁹

The small adjacent band at 1670 cm^{-1} was assigned to $\text{C}=\text{C}$ bond resulting from dehydrofluorination (removal of HF).²⁰ This band indicated the presence of polarons in the polymeric matrix.

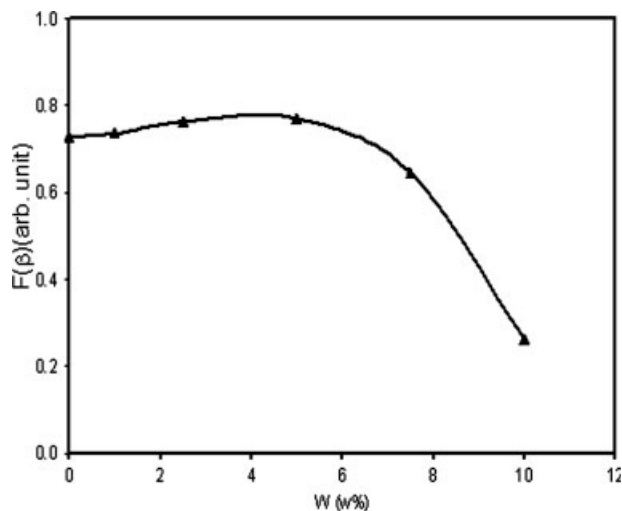


Figure 3 FL dependence of the relative intensity, $F(\beta)$.

The relative amount of the β phase, $F(\beta)$, that is, the ratio of the amount of the β phase to the total amount of the β and α phases, could be determined by using the peak transmittances at 510 cm^{-1} (for the β phase) and 765 cm^{-1} (for the α phase)²¹ through the equation $F(\beta) = A_{510}/(A_{510} + 1.26A_{765})$, developed by Osaki and Ishida.²² Figure 3 shows the FL dependence of the relative intensity, $F(\beta)$. It is clear that $F(\beta)$ was nearly constant up to $W = 5\%$; further increases in W resulted in a sharp drop in the $F(\beta)$.

X-ray diffraction

Figure 4 shows the X-ray diffraction (XRD) scans for various filling levels. The different crystal structures of PVDF (α , β , and γ phases) had similar peaks, but each phase had one or two peaks that made them identifiable. The most prominent peak for all phases occurred at approximately $2\theta = 20^\circ$. Table I lists the more prominent peaks observed in the PVDF diffraction scans.²³ No peaks corresponding to pure BiCl₃

TABLE I
Assigned X-ray Diffraction Peaks Characterizing α and β Crystalline PVDF Phases

W (wt %)	2θ ($^\circ$)	Assignment
0.0	18.4	(020) α
	20.0	(110) β
	26.8	(021) α
	39.2	(002) α
1.0	18.4	(020) α
	20.5	(110) β
	27.5	(021) α
	39.5	(002) α
2.5	20.6	(110) β
	27.8	(021) α
	32.9	(121) α
	39.8	(002) α
5.0	20.0	(110) β
	26.5	(021) α
	33.0	(130) α
	38.4	(002) α
7.5	21.0	(110) β
	26.8	(021) α
	33.9	(130) α
	38.4	(002) α
10	21.0	(110) β
	27.2	(021) α
	33.8	(130) α
	39.0	(002) α

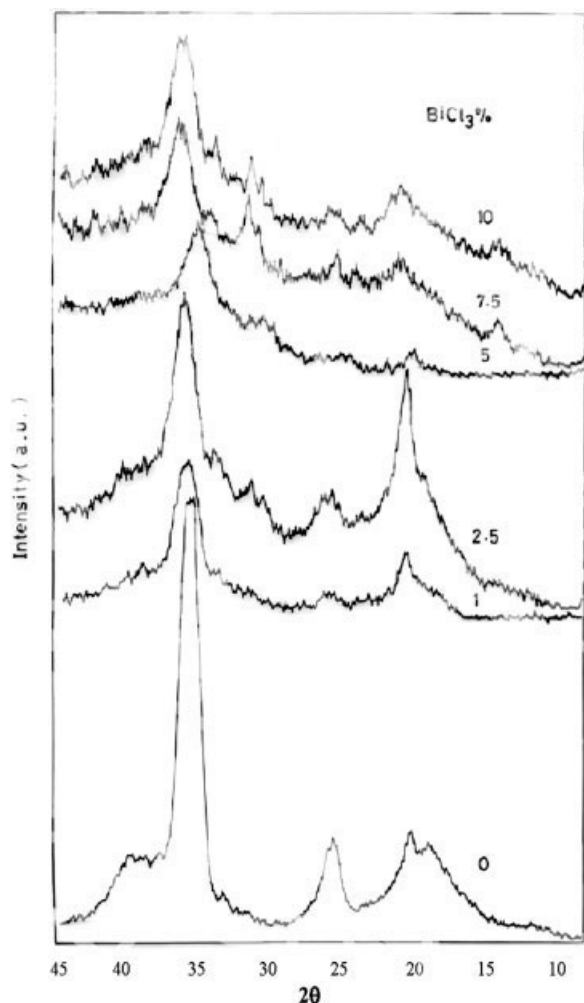


Figure 4 X-ray diffraction scans of PVDF filled with different FLs of various mass fractions of BiCl₃.

were found in the polymer composites, indicating complete dissolution of the compound in the polymer matrix.

The area under the peak, A_β , at $2\theta = 20.5^\circ$ can be taken as a measure of the degree of crystallinity for the β phase. Figure 5 shows the FL dependence of the area under the peak for the β phase. It is remarkable that the maximum value of A_β occurred at 2.5%, which is useful in some applications. This maximum confirmed the Fourier transform infrared analysis (FTIR) results. The decrease of the degree of crystallin-

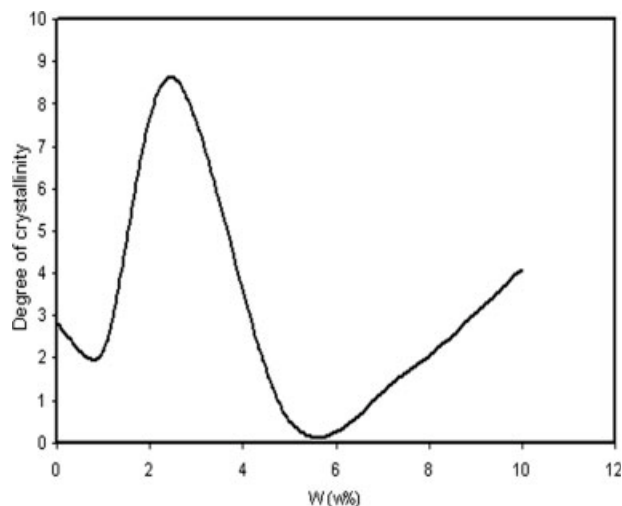


Figure 5 FL dependence of degree of crystallinity for the β phase at $2\theta = 20.5^\circ$.

ity for FL up to 2.5 wt.% can be explored by assuming that the excess BiCl_3 molecules may have attached to the PVDF chain via fluorine bridges. These results can be interpreted by considering the Hodge et al.²⁴ criterion, which establishes a correlation between the area of the peak and the degree of crystallinity.

Scanning electron microscopy

Scanning electron micrographs (SEMs) of the present system are displayed in Figure 6, which shows the microstructures of PVDF (dark area) and the filler (light area).²⁵ The SEMs suggest the FL dependence of the morphological structure.

The SEM of pure PVDF shows connecting uniform spherical domains with a pore shape. It was observed that the micrograph exhibited nearly the same morphology as that of pure PVDF, found previously in the literature.^{26,27} In contrast, the micrograph of $W=1\%$ was characterized by randomly distributed granules.

An interesting pattern was observed for $W=5\%$: a highly condensed number of small granules nearly equal in size.

The micrograph of the film of $W=7.5\%$ showed large granules and granule groups randomly distribution in a medium that appeared to be pure PVDF. The filler distributed uniformly in the polymeric matrix. Some pores between the polymer/filler interface could be observed, which was attributed to the partial

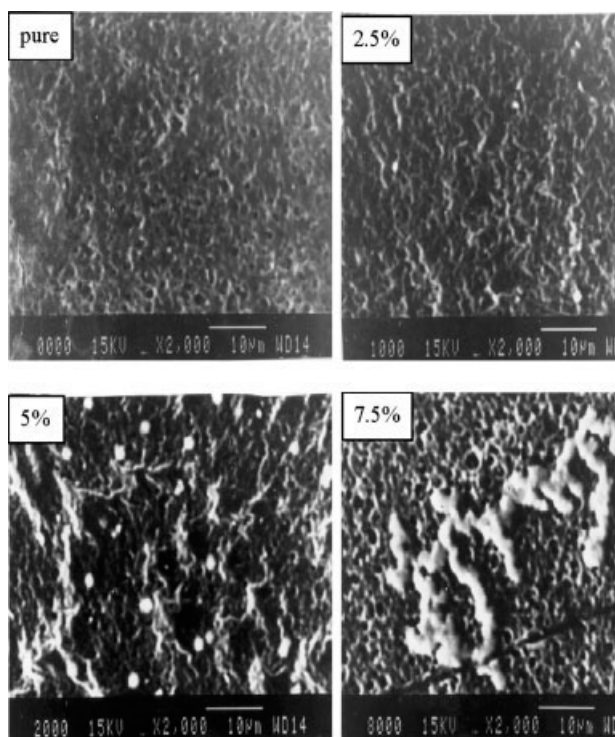


Figure 6 SEM micrographs of PVDF filled with various mass fractions of BiCl_3 .

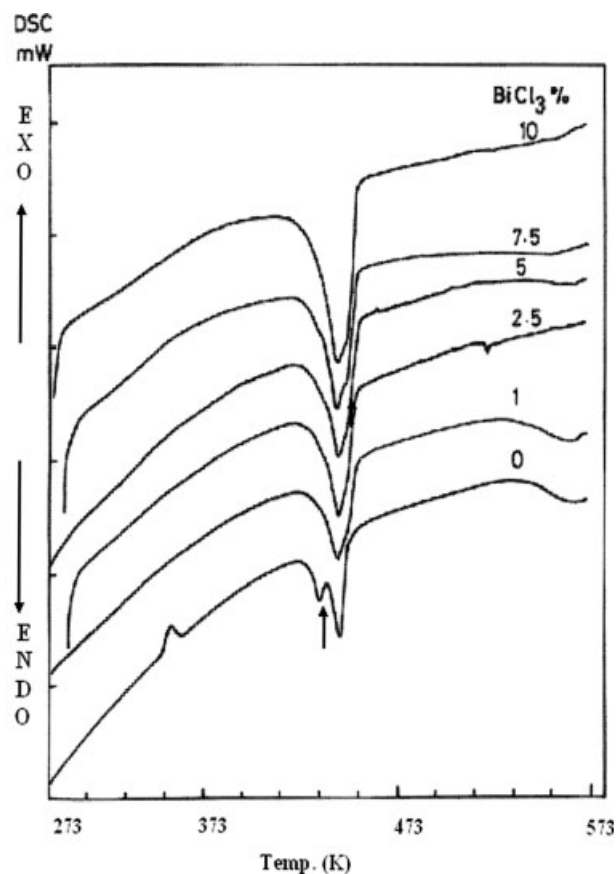


Figure 7 DSC thermograms of PVDF films filled with various mass fractions of BiCl_3 .

compatibility between the polymer and the filler. The 1% FL was found to be similar to pure PVDF and the 10% FL to be similar to 7.5% FL. Thus, the 1% and 10% micrographs are not presented.

Differential scanning calorimetry

The differential scanning calorimetry (DSC) thermograms of PVDF films filled with different FLs of BiCl_3 over the temperature range of 298–573 K are presented in Figure 7. A sharp endothermic peak was observed at $T_m = 444$ K because of the melting. The pure PVDF and some samples showed double melting peaks in the DSC scans.

There is considerable controversy in the literature about the double melting that takes place in many semicrystalline polymers. The origin of the double-melting peaks can be mainly ascribed to^{28–30}: (1) melting, recrystallization, and remelting during the DSC heating; (2) polymorphism; and (c) variation in morphology (lamellar thickness, perfection of crystals).

The order of reaction values, n , at T_m was calculated using the Kissinger method.³¹ The order of reaction values was $n \leq 1$. This indicates that most of the reactants were melted at T_m and that there was a small

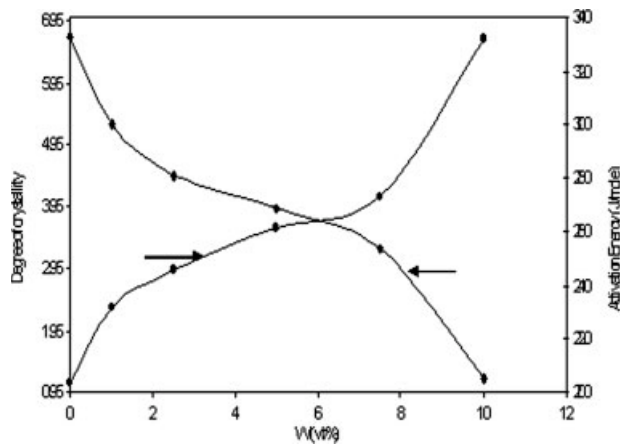


Figure 8 FL dependence of activation energy (◆) and degree of crystallinity (●).

amount of undecomposed reactants at T_m , supporting the multiplicity of the T_m peak.

The activation energy, E , was estimated by the Arrhenius equation³² using the melting peaks. The FL dependence of E is shown in Figure 8. It appears that the activation energy decreased with increasing FLs. From the melting thermogram, it was also possible to evaluate the area under the peak under consideration, and the degree of crystallinity could be calculated. The FL dependence of the degree of crystallinity is also shown in Figure 8. It was observed that the degree of crystallinity increased by increasing the FL.

DC electrical conduction

DC electrical resistivity (ρ) of the present samples was measured in the temperature (T) range of 300–400 K. The reciprocal temperature dependence of $\log \rho$, shown in Figure 9, did not exhibit an Arrhenius character. The mono- and/or difluorinated alkenes and the (h-to-h) and (t-to-t) polymer chain defects in the polymeric matrix of the present system, which

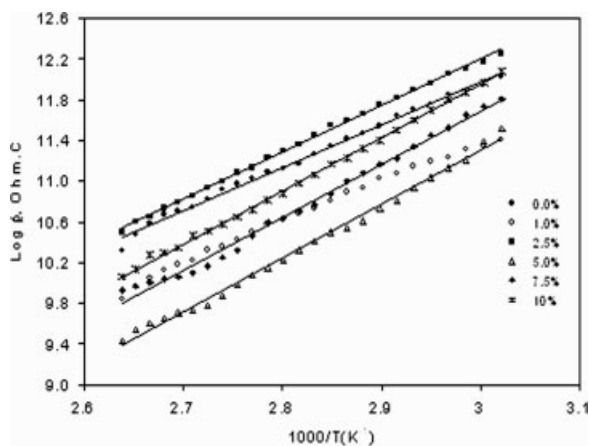


Figure 9 Reciprocal temperature dependence of $\log(\rho)$.

were evidenced by IR (band at 670 cm^{-1}), can be considered suitable sites for polarons and/or bipolarons. This allowed us to use the modified inter-polaron hopping model of Kuivalainen et al.³³ to interpret the present resistivity results. According to this model, conduction is attributed to a phonon-assisted charge carrier hopping between polaron and/or bipolaron bound states in the polymer. According to this model the electrical resistivity can be expressed as:

$$\rho = [kT/A_1 e^{\gamma(T)} (R_o^2/\xi)] \times \{[(y_p + y_{bp})^2 / y_b y_{bp}] [\exp(2B_1 R_o/\xi)]\} \quad (1)$$

where A_1 is 0.45; B_1 is 1.39; y_p and y_{bp} are the concentrations of polarons and bipolarons, respectively; R_o is $(3/4\pi C_{imp})^{1/3}$, which is the typical separation between impurities whose concentration is C_{imp} ; ξ is $(\xi_{||}\xi_{\perp}^2)^{1/3}$, which is the average decay length of a polaron and

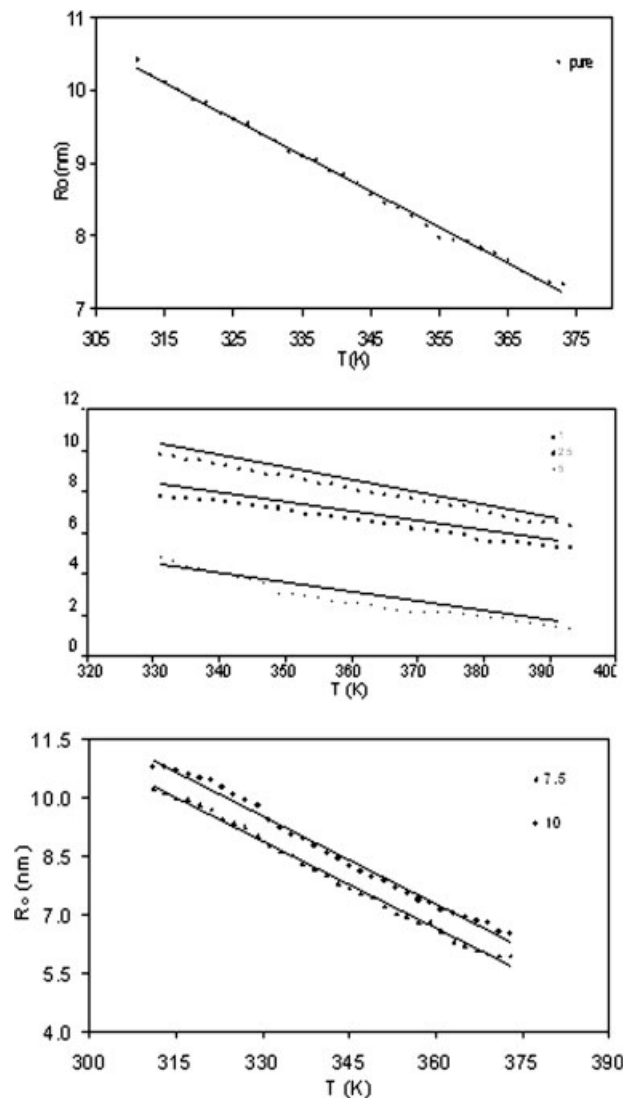


Figure 10 Temperature dependence of R_o .

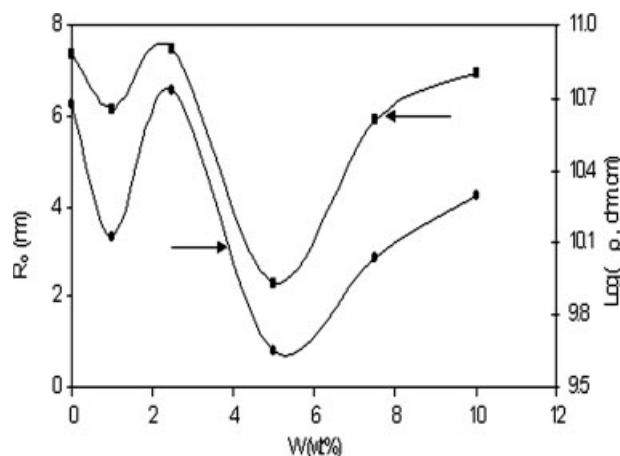


Figure 11 BiCl₃ FL dependence of log ρ (■) and R_0 (●) at $T = 373$ K.

bipolaron wave function, respectively; and ξ_{\parallel} and ξ_{\perp} are the decay lengths parallel and perpendicular to the polymer chain, respectively. Bredas et al.³⁴ reported that polarons and bipolarons induce defects of the same extension. The electronic transition rate between polaron and bipolaron states can be expressed as:

$$\gamma(T) = 1.2 \times 10^{17} (T/300 \text{ K})^{n+1} \quad (2)$$

where n is a constant of approximately 10, estimated by Kivelson.³⁵ In the present work the order of magnitude of ρ was adjusted using a computer-aided program. According to eq. (1), the plotting of log ρ versus reciprocal temperature, T , should give a straight line, if the measured ρ is dominated by polaron hopping. The parameter $\xi_{\parallel} = 1.06$ nm, whereas $\xi_{\perp} = 0.22$ nm,³⁶ which depends on the interchain resonance energy and the interchain distance.³⁷ Taking $y_b = y_{bp}$ for simplicity, which is an acceptable approximation,³⁸ and using eqs. (4) and (5), we can obtain the values of the hopping distance, R_0 .

The temperature and filling level dependences of R_0 are shown in Figure 10. A linear temperature dependence of R_0 was observed. It is remarkable that the calculated values of R_0 were in the range of 1.9–11 nm. Given that the monomer unit length was approximately 0.25 nm,³⁹ it could be observed that the hopping distance was in the range of 7.6–44 monomer unit lengths. This indicates that the present conduction mechanism was of an intrachain one-dimensional hopping type.

The FL dependence of log ρ and R_0 at a constant temperature ($T = 373$ K) is shown in Figure 11. It is remarkable that the logarithm of resistivity was in the range of 9.6–10.7 Ωcm .

It also was observed that the minimum value at $W = 5\%$ of log ρ and R_0 correlated with the

corresponding peak of the structural defect. Thus, the hopping process could be characterized especially by h-to-h as hopping sites.

CONCLUSIONS

The spectroscopic, thermal, electrical, and structural analyses of PVDF films filled with different FLs of BiCl₃ showed that:

- From IR analysis, the band at 1670 cm^{-1} was assigned to C=C stretching of the difluorinated. This band indicates the presence of polarons in the polymeric matrix. The maximum value of (h-to-h) was observed at 2.5%, which corresponded to the maximum values of the β phase at this FL supported by the X-ray analysis.
- XRD revealed two main characteristic peaks, at $2\theta = 20.5^\circ$ and 26° , for the α and β phases, respectively. No peaks corresponding to pure BiCl₃ were found, indicating complete dissolution of the compound in the polymer matrix. The maximum degree of crystallinity of the β phase occurred at 2.5% FL. This maximum confirmed the FTIR results. This maximum degree of crystallinity can be useful for several applications. The decrease in the degree of crystallinity for FL up to 2.5% can be explored by assuming that the excess of BiCl₃ molecules may have attached to PVDF chains via fluorine bridges.
- The SEM micrograph of pure PVDF showed connecting uniform spherical domains with a pore shape. An interesting pattern was observed for $W = 5\%$, which contained a highly condensed number of small granules nearly equal in size.
- The DSC revealed a sharp peak at $T_m = 444$ K because of melting. The origin of the double-melting peaks can be mainly ascribed to: (1) melting, recrystallization, and remelting during DSC heating; (2) polymorphism; and (3) variation in morphology.
- Electrical conduction was attributed to one mechanism of dimensional phonon-assisted charge carrier hopping between polaron and/or bipolaron bound states in the PVDF matrix.

References

1. Servet, B.; Ries, S.; Broussoux, D. *J Appl Phys* 1984, 55, 2763.
2. Hasegawa, R.; Takahashi, Y.; Chatani, Y.; Tadokoro, H. *Polym J*, 1972, 3, 600.
3. Takahashi, Y.; Matsubara, Y.; Tadokoro, H. *Macromolecules* 1983, 16, 1588.
4. Takahashi, Y.; Tadokoro, H. *Macromolecules* 1980, 13, 1317.
5. Hsu, S. L.; Lu, J. F.; Waldman, D. A.; Muthukumar, M. *Macromolecules* 1985, 18, 2583.
6. Takahashi, Y.; Matsubara, Y.; Tadokoro, H. *Macromolecules* 1982, 15, 332.

7. Takahashi, Y.; Tadakoro, H. *Macromolecules* 1980, 13, 1317.
8. Kepler, R. G.; Anderson, R. A. *J Appl Phys* 1978, 49, 8.
9. Meixner, H. *Ferroelectrics* 1991, 4, 279.
10. Tawansi, Y.; Abdelkader, H. I.; Balachandran, Y.; Abdelrazek, M. *J Mater Sci.* 1994, 29, 4001.
11. Naoto, T.; Yoshiaji, U.; Tsuyoshi, K. *J Appl Phys* 1993, 74, 3366.
12. Beaulieu, R.; Lessard, R. A.; Clim, S. L. *J Appl Phys* 1996, 79, 833.
13. Tawansi, A.; El-Khodary, A.; Zidan, H. M.; Badr, S. I. *Polym Testing* 2002, 21 381.
14. Tawansi, A.; Abdel-Kader, H. I.; Abdel-Razek, E. M.; Ayad, M. I. *J Mater Sci Technol* 1996, 13, 194.
15. Oraby, A. H. *Polym Testing* 2000, 19, 865.
16. Gregorio, R.; Captao, R. C. *J Mater Sci* 2000, 35, 299.
17. Kobayashi, M.; Tashiro, K.; Tadakoro, H. *Macromolecules* 1975, 8, 158.
18. Ostrovshii, D.; Brodin, A.; Torell, M.; Appetecchi, G. B.; Scrosati, B. *J Chem Phys* 1998, 109, 7618.
19. Crowderand, G. A.; Lightfoot, J. M. *J Mol Struct* 1983, 99, 77.
20. Nasef, M. M.; Saidi, H.; Dahlan, K. Z. *Polym Degr Stab* 2002, 75, 85.
21. Kim, K. J.; Cho, Y. J.; Kim, Y. H. *Vib Spectrosc* 1995, 9, 147.
22. Osaki, S.; Ishida, Y. *J Polym Sci, Polym Phys Ed* 1975, 13, 1071.
23. Davis, G. T.; McKinney, J. E.; Broadhurst, M. G.; Roth, S. C. *Macromolecules* 1978, 11, 1297.
24. Hodge, R. M.; Edward, G. H.; Simon, G. P. *Polymer* 1996, 37, 1371.
25. Ksy, R. P. *J Appl Phys* 1977, 48, 5301.
26. Rajendran, S.; Mahendran, O.; Mahalingan, T. *Eur Polym J* 2002, 38, 49.
27. Chen, N.; Hong, L. *Polymer* 2002, 43, 1429.
28. Blundell, D. J. *Polym* 1987 28, 2248.
29. Cheng, S. Z. D. *J Appl Polym Sci Polym Symp* 1989, 43, 315.
30. Chalmers, T. M.; Zhang, A. Q.; Shen, D. X.; Lien, S. H.; Tso, C. C.; Gabori, P. A.; Haris, F. W.; Cheng, S. Z. D. *Polym Int* 1993, 31, 261.
31. Kissinger, H. E. *Anal Chem* 1957, 29, 11.
32. Tawansi, A.; Oraby, A. H.; Badr, S. I.; Elashmawi, I. S. *Polym Int* 2004, 53, 377.
33. Kuivalainen, P.; Stubb, H.; Isotlo, H.; Yli, P.; Holmstrom, C. *Phys Rev* 1985, 31, 7900.
34. Bredas, J. L.; Chance, R. R.; Silbey, R. *Phys Rev* 1983, 26, 5843.
35. Kivelson, S. *Phys Rev* 1982, 25, 3798.
36. Mott, N. F.; Gurrey, R. W. *Electronic Processes in Ionic Crystals*; Oxford University Press: London, 1940; p 34.
37. Kivelson, S. *Phys Rev Lett* 1981, 46, 1344.
38. Tawansi, A.; Abdelkader, H. I.; Elzalabany, M.; Abdelrazek, E. M. *J Mater Sci* 1994, 29, 3451.
39. Sajkiewicz, P. *Eur Polym J* 1998, 35, 1581.